THE UNIVERSITY *of* EDINBURGH

Edinburgh Research Explorer

Functional inhibition of deep brain non-visual opsins facilitates acute long day induction of reproductive recrudescence in male Japanese quail

1   Running title: Deep brain photoreceptors in birds
2
3
4
5
6   **Title: Functional inhibition of deep brain non-visual opsins facilitates acute long day**
7   **induction of reproductive recrudescence in male Japanese quail.**
8
9
10

11 Authors: Jonathan H. Pérez*[1], Elisabetta Tolla[2], Valerie R. Bishop[3], Russell G. Foster[4], Stuart N.
12   Peirson[4], Ian C. Dunn[3], Simone L. Meddle[3], Tyler J. Stevenson[2].
13
14 Affiliation: 1. Biology Department, The University of South Alabama, Mobile Alabama, 36688,
15   USA.
16   2. Institute of Biodiversity, Animal Health and Comparative Medicine, University of
17   Glasgow, Glasgow G61 1QH, Scotland.
18   3. The Roslin Institute, The Royal (Dick) School of Veterinary Studies, University of
19   Edinburgh, Midlothian EH25 9RG, Scotland.
20   4. Sir Jules Thorn Sleep and Circadian Neuroscience Institute (SCNi) and Nuffield
21   Laboratory of Ophthalmology, Nuffield Department of Clinical Neurosciences,
22   Dorothy Crowfoot Hodgkin Building, University of Oxford, South Parks Road,
23   Oxford OX1 3QU.
24
25
26
27 *Corresponding author
28 Biology Department
29 The University of South Alabama
30 Mobile, AL 36688
31 5871 USA Dr
32 Email: jhperez@southalabama.edu
33 Phone: 251-460-6331
34
35
36 Disclaimer: The authors have nothing to disclose.
37
38
39
40 **Key words:** photoreceptor, VA opsin, neuropsin, OPN5, seasonality, reproduction, RNA

41 interference, viral vector

42

Highlights

- VA opsin and neuropsin RNAi silencing impact photoinduced activation of the reproductive axis in quail

- Effects of RNAi silencing of VA opsin and Opn5 variably impact reproductive axis activity

- Non-visual opsin photoreceptors appear to exert their effect at multiple points in the regulation of the reproductive axis.

Abstract

For nearly a century, we have known that brain photoreceptors regulate avian seasonal biology. Two photopigments, vertebrate ancient opsin (VA) and neuropsin (OPN5), provide a possible molecular substrate for this photoreceptor pathways. VA fulfills many criteria for providing light input to the reproductive response, but a functional link has yet to be demonstrated. This study examined the role of VA and OPN5 in the avian photoperiodic response of Japanese quail (*Coturnix japonica*). Non-breeding male quail were housed under short days (6L:18D) and received an intracerebroventricular infusion of adeno-associated viral vectors with shRNAi that selectively inhibited either VA or OPN5. An empty viral vector acted as a control. Quail were then photostimulated (16L:8D) to stimulate gonadal growth. Two long days significantly increased pituitary thyrotrophin-stimulating hormone β-subunit (*TSHβ*) and luteinizing hormone β-subunit (*LHβ*) mRNA of VA shRNAi treated quail compared to controls. Furthermore, at one week there was a significant increase, compared to controls, in both hypothalamic gonadotrophin releasing hormone-I (*GnRH-I*) mRNA and paired testicular mass in VA shRNAi birds. Opn5 shRNAi facilitated the photoinduced increase in *TSHβ* mRNA at 2 days, but no other differences were identified compared to controls. Contrary to our expectations, the silencing of deep brain photoreceptors enhances the response of the reproductive axis to photostimulation rather than preventing it. In addition, we show that VA opsin plays a dominant role in the light-dependent neuroendocrine control of seasonal reproduction in birds. Together our findings suggest the photoperiodic response involves at least twoAfter 7 days of photostimulation of VA opsin either directly co-expressed in GnRH-I neurons or indirectly (via disinhibition from VA neurons) resulted in higher GnRH expression and increased LHβ and FSHβ expression photoreceptor types and populations working together with VA opsin playing a dominant role.

Pérez et al., 3

Introduction

Annual changes in photoperiod, are the primary predictive cue regulating seasonal reproduction in many vertebrates (Dawson et al., 2001; Rowan, 1925). The photoperiodic response is a well characterized cascade of neuroendocrine changes that transition birds from a short day (SD) non-breeding to a long day (LD) reproductive state (Follett and Pearce-Kelly, 1991; MacDougall-Shackleton et al., 2009). Exposure to a single day of photoperiod exceeding 13 hours of light stimulates thyrotrophs in the pars tuberalis to release *TSHβ*, inducing a reciprocal switch in deiodinase gene expression in the MBH (Nakao et al., 2008). Continued long-term LD exposure maintains high GnRH-I synthesis in the preoptic area (POA) and permits GnRH-I release, to stimulate luteinizing hormone (LH) and follicle-stimulating hormone (FSH) release from the anterior pituitary gland.

In mammals, a discrete population of retinal ganglion cells, expressing the non-visual photoreceptor melanopsin (OPN4), are critical for transduction of seasonal light information (Foster et al., 2020; Hankins et al., 2008). However, in most non-mammalian species, light-driven changes in seasonal physiology occur via extra-retinal photoreceptors (Menaker et al., 1970; Menaker and Keatts, 1968; Pérez et al., 2019). Targeted illumination studies have localized the photoreceptors for avian reproduction to the medial basal hypothalamus (MBH) (Benoit and Ott, 1944; Oliver and Baylé, 1975). The action spectrum (λ_{max}) for reproductive photostimulation in Japanese quail (*Coturnix japonica*) established the involvement of an opsin/vitamin-A based photopigment with a maximum spectral response of ~492 nm (Foster et al., 1985; Foster and Follett, 1985). To date, three photoreceptor opsins have been characterized and localized within the hypothalamus of birds: vertebrate ancient opsin (VA; Halford et al., 2009), neuropsin (OPN5; Nakane et al., 2014) and melanopsin (OPN4; Chaurasia et al., 2005).

98   VA is expressed in the preoptic area (POA) and mediobasal regions of the hypothalamus

99   (Halford et al., 2009). Crucially, VA cells exhibit an absorption spectrum closely matching the

100   reproduction spectra maximum for reproductive physiology (~490nm; Davies et al., 2012) and

101   are co-localize with gonadotropin-releasing hormone I (GnRH-I) expressing cells (Halford et al.,

102   2009) providing a link between light detection and activation of the reproductive axis (García-

103   Fernández et al., 2015). However, a functional role for VA in the photoperiodic response has yet

104   to be demonstrated. OPN4 is expressed in the pre-mammillary nucleus of turkeys (*Meleagris*

105   *gallopavo*) (Kang et al., 2010), with very low OPN4 expression recently reported in the quail

106   infundibular hypothalamic region (Nakane et al., 2019). However, the lack of strong mediobasal

107   localization suggests that OPN4 is not likely to be the primary photoreceptor for reproduction in

108   birds (Peirson and Foster, 2006). Conversely, histological analyses have demonstrated that

109   OPN5-expressing cells are localized to the periventricular organ (PVO) within the mediobasal

110   hypothalamus. OPN5 cells project towards the pars tuberalis, a region involved in coordinating

111   GnRH-I release (Nakane et al., 2014), yet OPN5 has an absorption spectrum (420 nm);

112   considerably lower than the reported maxima of ~492nm for photoperiodic induction. Functional

113   studies have shown that RNA inhibition of OPN5 alters thyrotrophin-stimulated hormone β-

114   subunit (*TSHβ*), a key gene in the photostimulation of reproduction, expression in canaries

115   (*Serinus canaria*) (Stevenson and Ball, 2012), red-headed bunting (*Emberiza bruniceps*)

116   (Majumdar et al., 2014) and Japanese quail (Nakane et al., 2014). But OPN5 has not been linked

117   directly to other upstream components of the reproductive axis.

118   The three main components of the avian reproductive response are: i) deep brain

119   photoreceptor(s), ii) a circadian clock (Follett and Sharp, 1969) and iii) GnRH-I synthesis and

120   secretion (Stevenson et al., 2012). To date, only OPN5 has been functionally implicated in the

121 acute photoinduced regulation of *TSHβ*. No study has examined the functional role of VA, nor

122 the long-term role of any photoreceptor. To address this deficit in knowledge, the current study

123 aimed to establish any functional roles that VA and OPN5 opsins may play in the photoperiodic

124 regulation of reproduction in the Japanese quail. Short-hairpin RNA (shRNA) constructs

125 packaged in adeno-associated virus (AAV) were used to test the hypothesis that VA and/or

126 OPN5 are necessary for i) the short-term photoinduction of *TSHβ, GnRH-I, LHβ-subunit* and

127 *FSHβ-subunit* (*FSHβ)* mRNA expression, and ii) are involved in the development and

128 maintenance of photoinduced reproduction.

Materials and Methods

Ethical approvals

131 Animal procedures were approved by the Roslin Institute Animal Ethics and Welfare

132 Review Board at the University of Edinburgh and were performed under Home Office approval

133 (PPL P61FA9171). The experiments were designed in accordance with the Animal Research

134 Reporting of In Vivo Experiments (ARRIVE) guidelines and National Centre for the

135 Replacement, Refinement and Reduction of Animals in Research.

136

Adeno-associated viral vector, shRNA design and cellular expression

139

140 Custom adeno-associated virus serotype 2 vectors containing shRNA templates targeting

141 either OPN5 (*vOPN5*) or VA (*vVA*) were produced by Virovek (Hayward, CA). shRNAi

142 contained a hair-pin loop insert (TCAAGAG); both *vVA* and *vOPN5* targeted exon 4 (S1 Table

143 and Fig. 1A). To identify any potential off-target effects, Blastn search was conducted, no

144 sequences with high homology (>90%) were identified against the shRNAi. The low homology

145 aligned sequences identified by Blastn are not associated with regulation of the photoperiodic

146 response and nor expressed in the mediobasal hypothalamus, giving confidence that RNA

147 interference induced by the shRNAi constructs are highly specific for VA and OPN5.

148   shRNAi were expressed under a constituently active CMV promoter in an expression

149 cassette, which also contains green fluorescence protein (GFP) to facilitate infected cell

150 identification (Fig.1B). The CMV expression cassette was selected based on pilot tests using

151 primary cell culture to confirm the capability of AAV2 to successfully transfect and be expressed

152 in quail nervous tissue (Fig. 1).

153

Animals

155   All studies used adult (>12-week-old) male Japanese quail (*Coturnix japonica*) hatched

156 and reared at the National Avian Research Facility, University of Edinburgh, Scotland, UK until

157 at least 3 months of age. Birds were provided food and water *ad libitum*. Following rearing, birds

158 were transferred to short days (6L:18D; Lights on at 07:00) for at least 8 weeks to ensure all

159 birds were in a photosensitive, non-breeding condition (Follett and Pearce-Kelly, 1991).

160

Pilot testing of AAV2 vectors

162   To determine suitability of the AAV2 vector construct, primary cell culture testing using

163 neural explants from embryonic quail were conducted. The basal portion of a day 10 quail

164 embryo brain (10 days of incubation; quail hatch at E18) was explanted and homogenized to

165 generate a primary cell culture for testing. Explants were transferred to ice cold phosphate

166 buffered saline (PBS) and then cultured in sterile 24 well culture plates with 500 µl of incubation

167 media overnight at 37oC with 5% CO_2. Incubation media contained Dulbecco's Modified Eagle

168   Medium (DMEM; Fisher Scientific) base with 1% Penstrep and 10% fetal bovine serum (Fisher

169   Scientific). Following overnight incubation 400 ul of incubation media was removed and

170   replaced with 600 µl of fresh incubation media containing 4 µl, 2 µl, 1 µl or 0.5 µl of Virovek's

171   AAV2-CMV vector containing only GFP (Vector Labs, Hayward CA.; 2-2.5E+13 vg/100 ul).

172   Incubation media was refreshed daily and explants were cultured for five days prior to

173   fluorescent imaging. GFP presence or absence was determined by fluorescence microscopy

174   (Zeiss Axiovert 25 and 100 fluorescent microscopes with Axiocam 503c cameras running Zeiss

175   Zen software; Figure S1C). Both 4 µl and 2 µl doses of vector produced strong detectable signal

176   distinctly localized to individual cells, indicating reliable transfection.

177

Stereotaxic intracerebroventricular injection of shRNA-AAV2 vectors

178
179

180
181   AAV2 vectors were delivered via stereotaxic intracerebroventricular (ICV) injection into

182   the third ventricle (3V) of the medial basal hypothalamus (MBH). Injection coordinates were

183   refined from estimates taken from the adult quail brain atlas (Baylé et al., 1974) using test

184   injections of India ink into fresh quail cadavers. Following test injections, brains were removed,

185   frozen on dry ice and coronally sectioned on a cryostat at 50 µM. Sections were mounted to glass

186   microscope slides for rapid visualization via light microscopy. This process was repeated

187   iteratively to optimize the anatomical localization of injections directly into the MBH. The final

188   coordinates used were determined with respect to the bursa as X = 0.0 mm, y = 3.8 mm, and z = -

189   6.3 mm then pulled up to -6.0 mm for injection.

190   All experimental ICV injections were performed following standard protocols developed

191   in consultation with the Named Veterinary Surgeons using aseptic technique. Birds were

192 anesthetized with isoflurane (4-5%) administered by facemask with 1.5 L/min of O_2, following

193 induction of anesthesia Isoflurane was reduced to ~2%, monitored and adjusted continually by

194 the anesthetist to maintain desired anesthetic depth. Animals then received subcutaneous

195 injections of meloxicam (0.5 mg/kg) and butorphanol (1.5 mg/kg) as analgesia prior to

196 positioning in the stereotaxic frame (Kopf Instruments). Feathers were plucked and the surgical

197 site cleaned with Hibiscrub. A small ~1 cm incision was made by scalpel to expose the skull.

198 The tip of the injection syringe was aligned to the bursa and zeroed then moved to the injection

199 coordinates and a small mark placed with a pencil prior to clearing the syringe. A dental ball mill

200 drill bit (size #4; WPI) was used to drill a small hole (~ 1-2 mm in diameter) though the skull.

201 The syringe was then realigned and coordinates verified prior to insertion of the needle to target

202 coordinates. A 10 ul Hamilton syringe fitted with a sterilized 28-gauge microfillers (WPI

203 MF28G-5; 97mm, 0.35mm OD, 0.25mm ID) trimmed to half-length were used for injections.

204 Birds were injected with 1 μL of AAV2 at ~2.34E+13 vg/ml containing: blank cassette shRNAi

205 (control, CV), shRNAi vOPN5 or shRNAi vVA. The surgical incision was closed either by

206 veterinary adhesive (VetBond 3M) or sutures. Animals recovered in an isolated box before

207 transfer to a communal recovery pen, equipped with food, water and a heat lamp. The

208 photoperiod was lengthened by one-hour (7L:17D) to facilitate recovery.

209

Study 1: The effect of acute photoinduction and shRNAi on the hypothalamic-pituitary-gonadal axis

212   To establish a non-breeding baseline of target gene expression, as well as determine any

213 direct effects of the AAV2 vector, a subset of birds (n = 5) were injected with the CV vector

214 whilst kept on SD (7L:17D) for 2 weeks and then culled. Birds were closely monitored during

215 this period for signs of any adverse effects. All birds remained healthy and the main experiment

216 commenced.

217   To determine the effects of opsin silencing on the initial photoinduction of the

218 reproductive axis birds were injected with CV (n = 5), *vOPN5* (n = 5) or *vVA* (n = 8) held on

219 short days SD (7L:17D; lights on 07:00) for 2 weeks and then transferred to 16L:8D for 2 days

220 or 7 days (CV n= 6, *vOPN5* n = 9, *vVA* n= 7) prior to collection. Blood samples (≤ 250 µl) were

221 collected by venipuncture of the wing vein using a 26-gauge needle and collected from the

222 surface using heparinized microcapillary tubes. Blood was collected from all birds 2 days prior

223 to photostimulation and then again at cull (2 or 7 days). In total across treatments and time points

224 45 quail were used in the experiment (CV n=16, vOPN5 n=14, vVA n=15). Plasma was

225 separated by centrifuging the microcapillary tubes at 10,000 g for 5 minutes, aspirated and then

226 stored at -20°C until assay for testosterone. Birds were euthanized by cervical dislocation

227 followed by rapid decapitation between the hours of 10:00 and 12:00. This early phase of the

228 light-dark cycle was selected due the increased levels of gonadotropins identified previously

229 (Meddle and Follett, 1997, 1995). Brain and pituitary stalk tissues were rapidly dissected and

230 fresh frozen on dry ice. Both testes were dissected and weighed on an analytical balance (Sartoris

231 model A200S) to the nearest 0.1g. All tissues were stored at -80°C.

232

Study 2: The effect of chronic photostimulation and shRNAi on the photoperiodic response

235   To determine the effects of long-term opsin silencing a second study was conduct by

236 transferring birds from SD to LD for 28 days, a period well-established to stimulate maximal

237 gonadal growth (Follett and Pearce-Kelly, 1991). Birds were pseudo-randomly administered with

238 ICV shRNAi containing either i) CV (n= 8), or treatment groups that consisted of ii) *vVA* opsin

239   shRNAi (n= 9), or iii) *vOPN5* shRNAi (n= 9), then kept on a photoperiod of 7L:17D for 2 weeks

240   and then photostimulated (16L:8D). Blood samples ($\leq$ 250 µl) were collected as described above

241   2 days pre-photostimulation and then at 7, and 28 days following photostimulation. Blood was

242   centrifuged and plasma aspirated as above and stored at -20°C until assay. Tissues were

243   dissected and stored as described above.

244

Brain sectioning and AAV GFP histological localization

246   Brains from the second study were coronally sectioned at 30 µm, mounted onto polysine

247   slides (Fisher 10219280) and cover slipped with VECTASHIELD Antifade Mounting Media

248   with DAPI (Vector Labs, Burligame, CA USA). Slides were examined under fluorescence

249   microscopy to confirm localization of GFP signal to the MBH (Fig. 1). Birds where injections

250   were found to be off target, or there was no sign of injection were excluded from subsequent

251   analyses (see below).

252

Western Blot assays of hypothalamic extracts for VA and OPN5

254   Polyclonal antibodies against VA and OPN5 were custom made by Cambridge Research

255   Biochemicals, Inc. (see Supplemental Table 3 for target sequences) in rabbit hosts with sub-

256   fractions of collected sera purified via affinity chromatography. Antibody sequence target were

257   selected based on previously published specificity for VA (Halford et al., 2009) and OPN5

258   (Nakane et al., 2010). BLASTp analyses confirmed that the OPN5 sequence has 100% sequence

259   homology with the predicted OPN5 target and non-specific hits were <80% homology with

260 <80% coverage. For VA there was 100% identity and 100% coverage of the antibody sequence

261 for the Japanese quail sequence, confirming the high homology. Furthermore, there was low non-

262 specificity for off-target sequences with <80% identity and <80% coverage.

263   To confirm reduced VA and OPN5 protein expression, western blots were conducted on

264 hypothalamic protein extracts. The hypothalami were dissected (as described above) and

265 homogenized in 700 µl of 100 mM Tris-HCL buffer with 4% w/v SDS and protease inhibitors

266 (Halt™ Protease Inhibitor Cocktail, EDTA-free, Thermo Fisher Scientific). Samples were then

267 centrifuged at 20,000 x g for 20 minutes at 4°C. Supernatant was collected and stored at -80°C.

268 Total protein concentration for all samples was determined using 1 µl of supernatant using a

269 BCA Protein Assay (Pierce™ BCA Protein Assay Kit) per manufacturer's instructions.

270 Supernatant volume for use in western blots was then standardized to add 10 µg of protein to

271 each well by diluting with water. 20 µl of diluted sample was combined with 10 µl of LDS

272 buffer (NuPAGE™ LDS Sample Buffer, Thermo Fisher Scientific) then incubated at 98°C for 2

273 minutes prior to loading. Samples were loaded onto 4-12% Bis-Tris pre-cast gels (NuPAGE™,

274 Thermo Fisher Scientific), 10 µl per sample and were loaded onto two separate gels that were

275 run in parallel in the same gel tank. Treatment groups were spread across gels. Gels were run at

276 90V or 5 minutes to ensure even entry of samples into the gel, then at 175V for 1 hour. One

277 duplicate gel was then immediately incubated in 40 ml of OptiBlue protein stain for 1 hour, to

278 quantify total protein loading, on an orbital shaker. The second gel was then processed for

279 western blot transfer. Protein was transferred to a PDVF membrane (iBlot™ Transfer Stacks,

280 PVDF, regular size, Thermo Fisher Scientific) using the iBlot 2 system. Membranes were then

281 washed in 1X PBS 5 times for 5 minutes before being blocked for 30 minutes in Odyssey

282 blocking buffer in 50 ml falcon tubes. Blocking buffer was discarded and replaced with 5 ml of

283 primary antibody solution (5 ml Odyssey buffer, 1 AB, 0.1% Tween 20). Following primary

284 antibody incubation, samples were rinsed in PBS 6 times for 5 minutes. Incubation with

285 secondary antibody was performed using IRDye 680RD Goat Anti-Rabbit antibody (LI-COR) at

286 1:10,000 in 5 ml Odyssey Blocking Buffer with 0.1% Tween 20 before being incubated in

287 secondary antibody for 90 minutes at room temperature. Membranes were then rinsed with PBS

288 6 times for 5 minutes prior to imaging. Membranes were imaged on a LI-COR Odyssey imager

289 using Image Studio software (Image Studio™ LI-COR). Western blots were imaged at 3.5

290 intensity, medium image quality at 169 µm resolution. Total protein gels were rinsed in distilled

291 water and then imaged on the 700 nm channel at lowest image quality, Intensity 3, 169 µm

292 resolution.

293

Enzyme-linked immunosorbent assay (ELISA) for testosterone

295   To measure plasma testosterone levels, the Parameter™ Testosterone Assay (R&D

296 Systems, Bio-Techne) was used according to manufacturer's instructions. Samples were assayed

297 in duplicate using 50 µl plasma and absorbance was measured at 450 nm and 570 nm using a

298 microplate reader (LT-4500, Labtech). For each well, the value from 570 nm was subtracted

299 from the value for 450 nm to obtain a normalized fluorescent measurement. The sensitivity of the

300 assay ranged from 0.012-0.041 µg/ml. Cross-reactivity of the assay was <0.1% for androsterone,

301 estradiol, prednisolone and progesterone. Two assays were conducted, the intra-assay coefficient

302 of variation was 7.7% and 9.4%. The inter-assay coefficient of variation was 13%.

303

RNA isolation and cDNA synthesis

305   Hypothalami were dissected from the first study using well characterized

306   neuroanatomical landmarks (Baylé et al., 1974; Pérez et al., 2020). Hypothalami were then

307   homogenized in 700 µl of 100 mM Tris-HCL buffer with 4% w/v SDS and protease inhibitors

308   (Halt™ Protease Inhibitor Cocktail, EDTA-free, Thermo Fisher Scientific). Homogenized

309   samples were then centrifuged to pellet debris and the supernatant was then transferred to clean

310   microcentrifuge tubes for protein analysis (S1 File). Hypothalamic pellets and pituitary glands

311   were homogenized using 1 ml of TRIzol (Thermo Fisher Scientific) using a Kinematica Polytron

312   PT1200E handheld homogenizer (Thermo Fisher scientific). Following a 5minute room

313   temperature incubation, 200 µl of chloroform was added to each sample and vortexed to mix.

314   Samples were then incubated for 3 minutes at room temperature, then centrifuged at 12,000 g for

315   15 minutes at 4°C. The upper aqueous phase was pipetted into a fresh microcentrifuge tube. 500

316   µl of isopropanol was added and incubated for 10 minutes. Tubes were centrifuged again at

317   12,000 g for 15 minutes at 4°C. Supernatant was discarded and the pellet re-suspended in 1 ml of

318   75% ethanol. Samples were centrifuged at 7,500 g for 5 minutes at 4°C and supernatant

319   discarded. The remaining pellet containing the RNA was re-suspended in 30 µl of RNase-free

320   water. Nucleic acid quality (260/280) and concentration was determined by Nanodrop (Thermo

321   Fisher Scientific). 2 µg of RNA was reverse transcribed using a Precision nanoScript2 Reverse

322   Transcription kit (Primerdesign Ltd) following the manufacturer's instructions and cDNA was

323   stored at -20°C until quantification.

324

325 Real-time quantitative PCR (qPCR)

326   qPCRs were performed on a Stratagene Mx3000 Real Time PCR machine in 20 µl

327   reactions. For each well, the qPCR mix consisted of 5 µl cDNA template, 10 µl SYBR green

328 (Primerdesign Ltd), 0.5 µl (300nM) forward primer, 0.5 µl (300nM) reverse primer and 4 µl

329 RNase-free H2O. Samples were run in duplicate in a 96-well plate format under the following

330 conditions: i) denaturing at 95°C for 5 min., then 39 cycles of ii) 95°C for 10 s, iii) 30 s at

331 annealing temperature dependent on primer (See Table 2), and finally iv) an extension step of

332 72°C for 30 s. Melt curves were analyzed to ensure the specificity of each reaction. PCR

333 Miner (Zhao and Fernald, 2005) was used to determine reaction efficiencies and

334 quantification cycle (Ct). Fold expression was measured in relation to

335 the average Ct for two reference genes (*GAPDH* and *βACTIN*) and calculated using 2-

336 ($\Delta\Delta$Ct). The average Ct obtained from short day CV treatment group was used as the second

337 delta value in order to identify photoinduced changes in transcript levels.

338

Exclusion criteria

340   Some quail were excluded from statistical analyses based on both a priori exclusion

341 criteria and based on outlier testing during statistical analysis. For the first study, one short day

342 control bird, two CV and 3 *vOPN5* shRNAi treated birds were removed because testicular mass

343 values were indicative of breaking the non-breeding state (i.e. 1.4 - 3.2g) while still on short

344 days. Opsin silencing was confirmed by both Western Blot and qPCR to confirm high efficiency

345 of AAV2 vector delivery to MBH (S1G and S1H Fig). Two *vOPN5* and two *vVA* treated birds

346 were excluded from analyses due to mRNA expression values being similar to control treated

347 birds, as a consequence of off-target viral injections. One *vOPN5* bird was excluded from the

348 western blot validations because of a technical error in gel loading. In the second study birds

349 were screened for inclusion by presence of GFP signal in the MBH, taking advantage of the

350   AAV2 vector's GFP expression (independent of shRNA. One CV and one *vOPN5* were excluded

351   based on lack of GFP expression in the MBH. Raw data and R code are available in S2 File.

352

Statistical analyses

354   All statistical analyses were conducted in R v 4.0.2 (R Core Development Team, 2020)

355   using the following packages: car (Fox and Weisberg, 2019), emmeans (Lenth et al., 2018), grid

356   (Murrell, 2005), ggthemes (Arnold, 2017), ggpubr (Kassambara, 2019), and tidyverse (Wickham

357   et al., 2019). Paired testes mass was analyzed by linear model. Model assumptions were checked

358   by graphic visualization of residual outputs using the plot() function to confirm model fit.

359   Initially, RNA expression data failed to fit linear model assumptions even when log transformed,

360   therefore, these data were subsequently analyzed by generalized linear model using a gamma

361   distribution with a log link. Model fit was checked via visualization of model residuals; use of

362   gamma models improved model fit based on AIC. Main effects within the model were assessed

363   using a Likelihood Ratio Test.

364

Results

Long day stimulation of testicular growth

367   In order to determine the long-term functional role of VA and OPN5, SD photosensitive

368   birds received a single intracerebroventricular (ICV) injection of shRNAi constructs targeting

369   VA (*vVA*), OPN5 (*vOPN5*), or empty cassette (CV) and then after a two-week recovery, were

370   exposed to stimulatory photoperiods for either 2, 7 or 28 days. Testes mass was significantly

371   heavier 7 days post photostimulation in all birds (Fig 2A; $F_{1,37}=14.69$, $p<0.001$, partial $\eta^2 =$

372 0.562). There was no detectable interaction effect for days post photostimulation and ICV

373 injection ($F_{2,37}$=2.66, p=0.083, partial η^2 = 0.126). However, based on the loss of statistical power

374 (<0.8) due to imbalance in sample sizes across treatments, and following visual inspection of

375 plotted data, opted to investigate photoinduced increases in testes mass at 2, 7, and 28 days post-

376 photostimulation separately as well.

377

378 We found that 2 days following photostimulation there was no effect of shRNAi

379 silencing on testes mass ($F_{2,13}$=0.35, p=0.713, partial η^2 = 0.05). After 7 days of

380 photostimulation, shRNAi silencing resulted in a significant increase in testes mass ($F_{2,19}$=4.31,

381 p=0.029, partial η^2 = 0.312), with *vVA* injected birds having heavier testes compared to control

382 (CV) birds (t=-2.78, p=0.031, Cohen's d = 1.50) suggesting that *vVA* treatment facilitated the

383 photoperiod induced growth of testes. There was no difference detected at 7 days between

384 *vOPN5* and CV birds (t=-0.80, p=0.706, Cohen's d = 0.49) not *vVA* and *vOPN5* birds (t=-2.23, p

385 = 0.092, Cohen's d = 1.03). There was no significant difference in testes mass between birds that

386 received shRNAi against OPN5 or VA for 28 days compared to CV (Fig 2B; $F_{2,23}$=0.28,

387 p=0.761, partial η^2 = 0.024). These data indicate that shRNAi of VA facilitated the long day

388 photoinduced transition (i.e. day 7) to a fully photostimulated reproductive state, accelerating

389 gonadal growth, which was complete in all birds by 28 days regardless of treatment.

390

391 Long days increased plasma testosterone concentrations

392 As testosterone is the predominant hormone produced by the testes, we sought to identify

393 whether circulating concentrations would parallel long day induced increases in testes mass.

394 There was no significant effect of treatment on plasma testosterone following 2 days of LD (Fig

395   2C; LR $\chi2$=0.81, p=0.667, partial η^2 = -0.933) nor an interaction of shRNAi injection and days

396   post-photostimulation (LR $\chi2$=0.64, p=0.726, partial η^2 = 0.438). Testosterone significantly

397   increased from 2 to 7 days post-photoinduction (LR $\chi2$=104.70, p<0.001, partial η^2 = 0.938).

398   Chronic silencing had no effect on plasma testosterone after 28 days (LR $\chi2$=0.52, p=0.77,

399   partial η^2 = 0.941). The lack of an effect of shRNAi on plasma testosterone concentrations at 28

400   days suggests that VA and OPN5 do not regulate short-term, daily rhythms in reproductive

401   physiology and instead, confirms their role in the long-term photoperiodic response.

402

Long days and shRNAi increased hypothalamic GnRH-I expression

404   Next, we sought to determine the neuroendocrine mechanisms underlying the shRNAi

405   induced increase in testicular mass. Using quantitative PCR (qPCR) we examined hypothalamic

406   *GnRH-I* and *GnIH* expression. There was a significant interaction for hypothalamic *GnRH-I*

407   expression between injection and days post photoinduction (Fig 3A; LR χ^2=16.70, p<0.001,

408   partial η^2 = 0.996) as well as a significant main effect of ICV injection (LR χ^2=10.59, p=0.005,

409   partial η^2 = 0.929). Post hoc testing using Student's T distribution via the summary.glm()

410   function indicated a significant increase in hypothalamic *GnRH-I* expression in *vVA* birds at 7

411   days when compared to CV (t_{18}=2.25, p=0.037, Cohen's d = 1.121), no other differences were

412   detected. Conversely, *GnIH* expression did not change following either 2 or 7 LD (Fig 3B; LR

413     $\chi2$=2.81, p<0.094, partial η^2 = 0.261). There was also no effect of ICV injection (LR $\chi2$=0.29,

414   p=0.867, partial η^2 = 0.232) nor an interaction between injection and days post photoinduction

415   (Fig 3D; LR $\chi2$=0.99, p=0.610, partial η^2 = 0.853). Taken together, these data indicate that VA

416   either directly (Halford et al., 2009) or indirectly is involved in regulating the photoperiod

417   induced increase in testicular mass via the master neuropeptide for reproduction, GnRH-I.

418

Long days regulate anterior pituitary secretagogue expression

420   Next, we investigated whether gonadotroph release from the pituitary gland was

421 regulated by shRNAi of VA and OPN5. Using qPCR, we assessed the photoperiod induced

422 change in *LHβ*, *FSHβ*, and *TSHβ* expression in birds after 2, 7 and 28 days. There were no

423 significant effects of ICV injection (LR $\chi2$ = 0.43, p = 0.807, partial η^2 < 0.001), following LD

424 transfer, nor any interaction between injection and days of photostimulation (LR $\chi2$ = 1.55, p =

425 0.460, partial η^2 = 0.447). As the findings indicated increased variation in *LHβ* expression at 2

426 LD, the effect of shRNAi on 2- and 7 LD were examined separately. There was a significant

427 effect of ICV injection at 2 days (Fig 3C; LR $\chi2$=7.26, p=0.027, partial η^2 = 0.277) with *vVA*

428 injected birds having higher *LHβ* mRNA expression compared to CV birds (t=2.64, p=0.022,

429 Cohen's d = 0.283) indicating that *vVA* increased *LHβ* expression. There was no difference

430 between CV and *vOPN5* birds (t=0.72, p=0.487, Cohen's d = 0.100). Chronic silencing had no

431 effect on *LHβ* expression (Fig 3D LR $\chi2$=2.56, p=0.279, partial η^2 = -4.11). *vVA* and *vOPN5*

432 groups did not show a significant reduction in *FSHβ* expression at 2 days LD (Fig 3E; LR

433 $\chi2$=5.45, p=0.066, partial η^2 = 0.999). No effect of injection on *FSHβ* expression was detected

434 following 7 days (LR $\chi2$ = 1.47, p = 0.481, partial η^2 = 0.951) nor 28 days (Fig 3F; LR $\chi2$=2.16,

435 p=0.339, partial η^2 = 0.785) of photostimulation.

436

437   There was no effect of ICV injection nor a significant interaction when *TSHβ* expression

438 was modelled over the entirety of the SD, 2 LD and 7 LD period. Due to the significant variation

439 at 2 days, treatment days were analyzed separately. Based on Cook's distance analysis of the

440 initial *TSHβ* glm model (at 2 days) residuals a single data point was identified as an outlier

441 (2.503 for bird 1703 CV at 2 days) and removed. Re-running of the analysis indicated that both

442 *vVA* and *vOPN5* significantly increased *TSHβ* expression at 2 days (Fig 3G; LR χ^2=16.81,

443 p<0.001, partial η^2 = 0.614). Post hoc testing indicated a very weak effect of *vOPN5* (t_{12}=2.19,

444 p=0.050, Cohen's d = 0.02) and a moderate effect of *vVA* (t_{12}=4.35, p<0.001, Cohen's d = 0.571)

445 silencing, increasing *TSHβ* expression compared to controls. No effect of injection was detected

446 at either 7 LD (LR χ^2=1.08, p=0.584, partial η^2 = 0.619) nor following 28 LD (Fig 3H; LR

447 χ^2=1.51, p=0.469, partial η^2 = 0.455).

448

Discussion

450   We found that selective inhibition of VA opsin mRNA expression facilitated the

451 photoinduced increase of *TSHβ* and *LHβ* mRNA expression in quail. By 7 days, *GnRH-I* mRNA

452 levels and testes mass increased in *vVA* treated birds compared to controls. Birds treated with

453 shRNAi against OPN5 were only observed to show increased *TSHβ* expression during early

454 photostimulation (2 days). Silencing treatment inhibited both VA and OPN5 opsin expression

455 and reduced associated protein levels with the exception of a transient increase in VA opsin at 2

456 days of photostimulation. Overall, these represent the first causal evidence that VA opsin plays a

457 functional role in the light-dependent neuroendocrine control of seasonal reproduction in birds.

458 However, contrary to our a priori hypotheses, silencing of deep brain photoreceptors enhances

459 the response of the reproductive axis to photostimulation rather than preventing it. This

460 challenges our previous understanding of the functional role of deep brain photoreceptors in the

461 activation of the reproductive axis (Fig 4).

462

463   This study provides the first long-term functional investigation of the hypothalamic

464   photoreceptors underpinning seasonal reproduction in birds. Previous studies have focused on

465   the well-characterized first LD release model to examine the impact of short-term inhibition of

466   OPN5 on photoinduced changes in *TSHβ* expression (Nakane et al., 2014; Stevenson and Ball,

467   2012), but have not explored long-term changes in neuroendocrine gene expression. In this

468   study, long-term inhibition of VA and OPN5 was achieved using adeno-associated viral

469   constructs (Nectow and Nestler, 2020). Using shRNAi, we are able to overcome the limitations

470   and potential detrimental impacts associated with use of systemic genetic knockouts (also not

471   currently available in quail) or lesions. By targeting both the early (i.e. 2-7 days) and late stages

472   (i.e. 28 days) of photostimulation our study aimed to monitor photoperiod induced changes at

473   genetic, physiological and morphological levels across time. Our findings expand our

474   understanding of the mechanisms regulating the avian photoperiodic response, identifying the

475   long-term impacts of VA and OPN5 inhibition on the neuroendocrine circuit that governs

476   testicular growth and function. However, as the complex differential response of the various

477   elements of the neuroendocrine cascade to silencing observed here highlights, transduction of

478   photic cues is a multi-modal process relying on multiple receptor types and likely multiple

479   receptor populations (Stevenson et al., 2022). These features make it challenging to isolate the

480   full role of even a single photoreceptor type in detail.

481

VA as a multi-modal photoreceptor for the avian photoperiodic response

482
483

484

485   Our findings identified that *vVA* significantly increased both TSHβ and LHβ at 2 LD.

486   Subsequently, GnRH-I and paired testes mass were increased at 7 LD. Interestingly, VA opsin is

487   closely related to the visual opsins phylogenetically (Beaudry et al., 2017; Soni et al., 1998);

488   both are within the subfamily of photoreceptors that activate intracellular Gα proteins by

489   catalyzing the exchange of GDP to GTP (Shichida and Matsuyama, 2009). Activation of

490   photoreceptors that couple the Gt subtype (i.e. rods, VA) generally decrease intracellular cGMP.

491   The second-messenger intracellular enzyme cyclic guanosine monophosphate (cGMP) has been

492   shown to bind to a 1.5kb enhancer motif upstream of the *GnRH-I* promoter repressing

493   transcription (Belsham et al., 1996). One potential link between light detection by VA opsin and

494   *GnRH-I* expression is via the direct action of cGMP and associated intracellular signaling

495   pathways. Immunohistochemical studies have demonstrated co-localization of VA and GnRH-I

496   in GnRH-I expressing neurons, in the anterior regions of the hypothalamus (García-Fernández et

497   al., 2015; Halford et al., 2009). Thus, we would expect tonic repression of *GnRH-I* expression in

498   these neurons that is released upon activation of VA opsin, based on the general mechanism of

499   action for opsin proteins. How then is it that silencing of the releaser, VA opsin, results in

500   upregulation of *TSHβ* and *LHβ mRNA* expression after 2 LD and particularly increased *GnRH-I*

501   expression and paired testes mass at 7 LD? The answer likely lies in the pathways that link VA

502   opsin to cGMP and *GnRH-I* transcription, and also the broad distribution of VA opsin within the

503   hypothalamus, where it has been identified in multiple nuclei (García-Fernández et al., 2015;

504   Halford et al., 2009). Co-expression of GnRH-I and VA opsin is limited primarily to anterior

505   nuclei: nucleus magnocellularis preopticus, nucleus anterior medialis hypothalamic, and the

506   nucleus supraopticus. Previous neuroanatomical analyses in European starling established that

507   the rostral preoptic area as the primary location of photoperiodic and gonadal hormone feedback

508   regulation on GnRH-I expression (Stevenson et al., 2009). However, there is also substantial VA

509   expression in the nucleus paraventricularis magnocellularis (both pars ventralis and medialis;

510 PVN) and the medial bed nucleus of stria terminalis with VA-ir positive fibers projecting into the

511 median eminence with an apparent interface with the PT (Halford et al., 2009). These two VA

512 opsin populations have the potential to independently regulate GnRH neuronal function and

513 GnRH-I release. Our ICV injections were targeted to the 3V in the medial basal hypothalamus to

514 optimize targeting of the PVN and ME, which contain both VA and OPN5 expression. Given the

515 targeting of our injections, the spread of GFP expression and the fact we still detected some level

516 of VA protein expression (Fig. 1) in our hypothalamic extracts, we posit that we were far more

517 effective at silencing MBH expression than anterior hypothalamic expression of VA opsin.

518 Based on this supposition and the anatomical localization of GnRH-I and VA opsin describe

519 above we suggest that VA acts in a modular manner to regulate different aspects of GnRH-

520 dependent control of reproductive physiology.

521 VA opsin neurons in the MBH project fibers through the ME to the PT allowing for direct

522 interaction with PT based thyrotrophs. Silencing of VA expression in these cells results in the

523 premature activation of these thyrotrophs resulting in the observed increase in *TSHβ* expression

524 at 2D. Work in sheep has suggested anterograde signaling from the PT directly to the pars

525 distalis of the anterior pituitary with respect to seasonal regulation of prolactin (Lincoln, 2002).

526 Anterograde signaling from the PT to pars distalis gonadotrophs provides a plausible mechanism

527 for the observed 2D elevation of *LHβ* in the vVA group. This model suggests some sort of

528 inhibition of PT thyrotrophs by this population of VA neurons that is released by removing the

529 opsin, likely requiring interaction with endogenous timing mechanisms. This population of VA

530 neurons is anatomically positioned to provide indirect regulation of the reproductive axis via the

531 canonical PT TSHβ to DIO2 pathway, potentially regulating GnRH release via modulation of

532 tanycyte endfeet interaction with the GnRH-I nerve terminal (Yamamura et al., 2004). At present

533   there is no clear mechanism by which this would occur in VA expressing neurons, but the

534   proposed model provides a framework to further investigate the molecular and microcircuit

535   mechanisms involved.

536   Conversely, the second major population of VA expressing neurons in the anterior

537   portion of the hypothalamus appears to be the GnRH-I neurons themselves, opening the potential

538   for direct regulation of GnRH-I by VA opsin. Based of our GFP localization data we suggest that

539   this population of VA opsin experienced reduced silencing and potentially remained functionally

540   intact. Thus, photostimulation of VA opsin expression in these neurons is expected to have the

541   effect of increasing GnRH-I expression by reducing cGMP as described above. Taken together

542   with the above findings a timeline of VA activity can be formulated, suggesting that the

543   photoinducible phase involves a VA -dependent increase in *TSHβ* and the subsequent stimulation

544   of *LHβ* within 2 days of LD transfer mediated by the MBH populations of VA opsin expressing

545   neurons. Simultaneously, VA opsin expressed in GnRH-I neurons modulates GnRH-I expression

546   to support sustained release of GnRH-I triggered by the TSHβ induced conformational changes

547   in ventricular tanycytes. The enhancement of reproductive physiology induced by VA silencing,

548   supported by prolonged suppression of VA mRNA, suggests that MBH VA expressing cells may

549   be acting as a brake upon an otherwise active reproductive system, preventing its activation.

550   Under this model LD exposure results in the removal of inhibitory tone on pars tuberalis

551   thyrotrphs beginning the neuroendocrine cascade events leading to reproduction. However,

552   despite the consistent and reliable reduction in VA mRNA for several weeks we observed a

553   transient increase in VA opsin protein on day 2 of photostimulation (Fig. 1F). Increased VA

554   opsin protein may have resulted in a larger pool of receptors in the MBH to detect light at day 2.

555   Therefore our results may be alternatively explained by stimulatory activation of VA opsin cells

556 in the MBH early in the photoperiodic response that facilitated gonadal growth. However, under

557 this explanation we might expect a subsequent decrease in gonadal growth later in

558 photostimulation when VA opsin protein levels were reduced, which we do not see. Overall, the

559 data reported herein provides the first functional evidence that VA opsin is integral to the

560 photoperiodic response in birds. The precise mechanisms linking VA opsin to gonadotrophin

561 release remain to be resolved, though it is clear that VA opsin influences GnRH-I mediated

562 regulation of reproductive physiology on the scale of days to weeks.

563

564

565   .

566

567 ## OPN5 as a mediator of the initial photoperiodic response

568   The findings presented here also support a functional role for OPN5 in the initial light-

569 dependent activation of seasonal reproduction. The current experimental design sought to

570 identify the effects of OPN5 inhibition on pituitary secretagogue (i.e. *LHβ*, *FSHβ*) expression,

571 identified as occurring early on the second LD in quail (Meddle and Follett, 1997). Early

572 morning tissue collection limits comparisons with previous studies, which utilized later evening

573 collections (Nakane et al., 2014; Stevenson and Ball, 2012). However, *TSHβ* expression was

574 increased after 2 LD in *vOPN5* treated birds. These data are similar to reports from Border

575 canaries in which shRNAi against OPN5 resulted in higher *TSHβ* expression 14 hours after light

576 onset on the first LD (Stevenson and Ball, 2012). Interestingly, in the present study we do not

577 find a clear long-term effect of *vOPN5* treatment on the HPG axis, suggesting that light

578 activation of this photoreceptor has only a short-term effect on the photoperiodic response

579 limited to the first days following LD stimulation. Collectively, these data suggest that activation

580 of OPN5 expressing cells is likely critical for early light detection and initiation of short-term

581 effects on the avian photoperiodic response, but that longer term effects are dependent on input

582 from other photoreceptors such as VA opsin.

583

584 Hierarchical organization of light detection by avian deep brain
585 photoreceptors

586 In the quail hypothalamus, VA mRNA and protein expression is 2x and 20x higher than OPN5

587 respectively. In addition VA cells are identified in several nuclei and have immunoreactive fibers

588 extend into multiple hypothalamic regions, in addition to the median eminence (Halford et al.,

589 2009). The observed robust and long-term effects of *vVA* on multiple neuroendocrine substrates

590 presented here suggest a predominant role for VA in the avian photoperiodic response, though

591 whether via stimulatory pathways of removal of inhibitory tone remains to be confirmed.

592 Furthermore, the VA action spectrum has the closest match to the action spectrum for the quail

593 photoperiodic response and is the only photoreceptor to meet all the criteria set forth for the

594 avian photoperiod response (García-Fernández et al., 2015). Therefore, we propose that light

595 detection by VA expressing cells in the MBH is the primary mechanism for acute (1st week LD)

596 photoinduction of reproductive physiology. However, it is likely that other photoreceptors, such

597 as anterior hypothalamic VA opsin, OPN5 or perhaps even OPN4 provide additional input to

598 facilitate the activation of the HPG axis.

599

600   A synthesis of the present and past studies highlights the complexity of opsin regulation

601 of seasonal reproduction (Pérez et al., 2019). Combining our data with this past synthesis we

602 propose a model of seasonal photoreception in which OPN5 expressing ependymal cells and

603 MBH VA cells regulate the initial response to photostimulation during the first long day by

604 acting on *TSHβ* expressing cells in the pars tuberalis to increase *TSHβ* expression (Nakane et al.,

605 2014; Stevenson and Ball, 2012). Simultaneously, VA expressing neurons in the preoptic

606 area/mediobasal hypothalamus respond to light stimulation over several days to weeks,

607 stimulating an increase in GnRH-I expression necessary to support long term activation of the

608 reproductive axis (Fig 4). Under this paradigm, VA serves as a long-term regulator, maintaining

609 the response to light and leading ultimately to reproductive competence. Whether these pathways

610 act completely independently or interact either directly, or indirectly, remains unclear at present.

611 Further work is needed to test the model proposed above and determine whether the involvement

612 of multiple opsins represents evolutionary redundancy or is a mechanism for enabling increased

613 flexibility and control of reproductive timing.

614

615

Acknowledgements

619

References

621 Arnold, J.B., 2017. ggthemes: Extra themes, scales and geoms for '"ggplot2."'R package version

622   3.4. 0.

623 Baylé, J., Ramade, F., Oliver, J., 1974. Stereotaxic topogrphy of the brain of the quail (Coturnix

624   coturnix japonica). J. Physiol. 68, 219–241.

625 Beaudry, F.E.G., Iwanicki, T.W., Mariluz, B.R.Z., Darnet, S., Brinkmann, H., Schneider, P.,

626   Taylor, J.S., 2017. The non-visual opsins: eighteen in the ancestor of vertebrates,

627   astonishing increase in ray-finned fish, and loss in amniotes. J. Exp. Zool. Part B Mol. Dev.

628   Evol. 328, 685–696. https://doi.org/10.1002/jez.b.22773

629 Belsham, D.D., Wetsel, W.C., Mellon, P.L., 1996. NMDA and nitric oxide act through the

630   cGMP signal transduction pathway to repress hypothalamic gonadotropin-releasing

631   hormone gene expression. EMBO J. 15, 538–547.

632 Benoit, J., Ott, L., 1944. External and Internal Factors in Sexual Activity 17.

633 Chaurasia, S.S., Rollag, M.D., Jiang, G., Hayes, W.P., Haque, R., Natesan, A., Zatz, M., Tosini,

634   G., Liu, C., Korf, H.W., Iuvone, P.M., Provencio, I., 2005. Molecular cloning, localization

635   and circadian expression of chicken melanopsin (Opn4): Differential regulation of

636   expression in pineal and retinal cell types. J. Neurochem. 92, 158–170.

637   https://doi.org/10.1111/j.1471-4159.2004.02874.x

638 Davies, W.I.L., Turton, M., Peirson, S.N., Follett, B.K., Halford, S., Garcia-Fernandez, J.M.,

639   Sharp, P.J., Hankins, M.W., Foster, R.G., 2012. Vertebrate ancient opsin photopigment

640   spectra and the avian photoperiodic response. Biol. Lett. 8, 291–294.

641   https://doi.org/10.1098/rsbl.2011.0864

642 Dawson, A., King, V.M., Bentley, G.E., Ball, G.F., 2001. Photoperiodic control of seasonality in

643   birds. J. Biol. Rhythms 16, 365–380. https://doi.org/10.1177/074873001129002079

644 Follett, B.K., Pearce-Kelly, A.S., 1991. Photoperiodic induction in quail as a function of the

645   period of the light-dark cycle: implications for models of time measurement. J. Biol.

646   Rhythms 6, 331–341.

647 Follett, B.K., Sharp, P.J., 1969. Circadian rhythmicity in photoperiodically induced

648   gonadotrophin release and gonadal growth in the quail. Nature 223, 968–971.

649   Foster, R.G., Follett, B.K., 1985. The involvement of a rhodopsin-like photopigment in the

650   photoperiodic response of the Japanese quail. J. Comp. Physiol. A 157, 519–528.

651   https://doi.org/10.1007/BF00615153

652   Foster, R.G., Follett, B.K., Lythgoe, J.N., 1985. Rhodopsin-like sensitivity of extra-retinal

653   photoreceptors mediating the photoperiodic response in quail. Nature 313, 50–52.

654   https://doi.org/10.1038/313050a0

655   Foster, R.G., Hughes, S., Peirson, S.N., 2020. Circadian Photoentrainment in Mice and Humans.

656   Biology (Basel). 9, 180.

657   Fox, J., Weisberg, S., 2019. An R Companion to Applied Regression, Third Edit. ed. Sage.

658   García-Fernández, J.M., Cernuda-Cernuda, R., Davies, W.I.L., Rodgers, J., Turton, M., Peirson,

659   S.N., Follett, B.K., Halford, S., Hughes, S., Hankins, M.W., Foster, R.G., 2015. The

660   hypothalamic photoreceptors regulating seasonal reproduction in birds: A prime role for VA

661   opsin. Front. Neuroendocrinol. 37, 13–28. https://doi.org/10.1016/j.yfrne.2014.11.001

662   Halford, S., Pires, S.S., Turton, M., Zheng, L., González-Menéndez, I., Davies, W.L., Peirson,

663   S.N., García-Fernández, J.M., Hankins, M.W., Foster, R.G., 2009. VA Opsin-Based

664   Photoreceptors in the Hypothalamus of Birds. Curr. Biol. 19, 1396–1402.

665   https://doi.org/10.1016/j.cub.2009.06.066

666   Hankins, M.W., Peirson, S.N., Foster, R.G., 2008. Melanopsin: an exciting photopigment.

667   Trends Neurosci. 31, 27–36.

668   Kang, S.W., Leclerc, B., Kosonsiriluk, S., Mauro, L.J., Iwasawa, A., El Halawani, M.E., 2010.

669   Melanopsin expression in dopamine-melatonin neurons of the premammillary nucleus of

670   the hypothalamus and seasonal reproduction in birds. Neuroscience 170, 200–213.

671   https://doi.org/10.1016/j.neuroscience.2010.06.082

672   Kassambara, A., 2019. ggpubr:"ggplot2" based publication ready plots. R package version 3.4.0.

673   Lenth, R., Singmann, H., Love, J., Buerkner, P., Herve, M., 2018. Emmeans: Estimated marginal

674   means, aka least-squares means. R Packag. version 1, 3.

675   Lincoln, G.A., 2002. Neuroendocrine regulation of seasonal gonadotrophin and prolactin

676   rhythms: lessons from the Soay ram model. Reprod. Suppl. 59, 131–147.

677   MacDougall-Shackleton, S.A., Stevenson, T.J., Watts, H.E., Pereyra, M.E., Hahn, T.P., 2009.

678   The evolution of photoperiod response systems and seasonal GnRH plasticity in birds.

679   Integr. Comp. Biol. 49, 580–589.

680   Majumdar, G., Yadav, G., Rani, S., Kumar, V., 2014. A photoperiodic molecular response in

681   migratory redheaded bunting exposed to a single long day. Gen. Comp. Endocrinol. 204,

682   104–113. https://doi.org/10.1016/j.ygcen.2014.04.013

683   Meddle, S.L., Follett, B.K., 1997. Photoperiodically Driven Changes in Fos Expression within

684   the Basal Tuberal Hypothalamus and Median Eminence of Japanese Quail.

685   Meddle, S.L., Follett, B.K., 1995. Photoperiodic activation of Fos-like immunoreactive protein in

686   neurones within the tuberal hypothalamus of Japanese quail. J. Comp. Physiol. A 176, 79–

687   89. https://doi.org/10.1007/BF00197754

688   Menaker, M., Keatts, H., 1968. Extraretinal Light Perception In The Sparrow, II. Photoperiodic

689   Stimulation of Testis Growth*. Proc. Natl. Acad. Sci. 60, 146–151.

690   https://doi.org/10.1073/pnas.60.1.146

691   Menaker, M., Roberts, R., Elliott, J., Underwood, H., 1970. Extraretinal Light Perception in the

692   Sparrow, III: The Eyes Do Not Participate in Photoperiodic Photoreception*.

693   Murrell, P., 2005. R Graphics. Chapman & Hall/CRC Press.

694 Nakane, Y., Ikegami, K., Ono, H., Yamamoto, N., Yoshida, S., Hirunagi, K., Ebihara, S., Kubo,

695   Y., Yoshimura, T., 2010. A mammalian neural tissue opsin (Opsin 5) is a deep brain

696   photoreceptor in birds. Proc. Natl. Acad. Sci. U. S. A. 107, 15264–15268.

697   https://doi.org/10.1073/pnas.1006393107

698 Nakane, Y., Shimmura, T., Abe, H., Yoshimura, T., 2014. Intrinsic photosensitivity of a deep

699   brain photoreceptor. Curr. Biol. 24, R596–R597. https://doi.org/10.1016/j.cub.2014.05.038

700 Nakane, Y., Shinomiya, A., Ota, W., Ikegami, K., Shimmura, T., Higashi, S.I., Kamei, Y.,

701   Yoshimura, T., 2019. Action spectrum for photoperiodic control of thyroid-stimulating

702   hormone in Japanese quail (Coturnix japonica). PLoS One 14, 1–15.

703   https://doi.org/10.1371/journal.pone.0222106

704 Nakao, N., Ono, H., Yamamura, T., Anraku, T., Takagi, T., Higashi, K., Yasuo, S., Katou, Y.,

705   Kageyama, S., Uno, Y., Kasukawa, T., Iigo, M., Sharp, P.J., Iwasawa, A., Suzuki, Y.,

706   Sugano, S., Niimi, T., Mizutani, M., Namikawa, T., Ebihara, S., Ueda, H.R., Yoshimura, T.,

707   2008. Thyrotrophin in the pars tuberalis triggers photoperiodic response. Nature 452, 317–

708   322. https://doi.org/10.1038/nature06738

709 Nectow, A.R., Nestler, E.J., 2020. Viral tools for neuroscience. Nat. Rev. Neurosci. 21, 669–681.

710 Oliver, J., Baylé, J.D., 1975. Multiple Unit Activity Patterns of Neuronal Populations in

711   Gonadotropic Areas of the Quail Hypothalamus: Spontaneous and Photically-Induced

712   Firing. Neuroendocrinology 17, 175–188. https://doi.org/10.1159/000122353

713 Peirson, S., Foster, R.G., 2006. Melanopsin: another way of signaling light. Neuron 49, 331–339.

714 Pérez, J.H., Swanson, R.E., Lau, H.J., Cheah, J., Bishop, V.R., Snell, K.R.S., Reid, A.M.A.,

715   Meddle, S.L., Wingfield, J.C., Krause, J.S., 2020. Tissue-specific expression of 11β-HSD

716   and its effects on plasma corticosterone during the stress response. J. Exp. Biol. 223.

717   https://doi.org/10.1242/jeb.209346

718   Pérez, J.H., Tolla, E., Dunn, I.C., Meddle, S.L., Stevenson, T.J., 2019. A Comparative

719   Perspective on Extra-retinal Photoreception. Trends Endocrinol. Metab. 30, 39–53.

720   https://doi.org/10.1016/j.tem.2018.10.005

721   Rowan, W., 1925. Relation of light to bird migration and developmental changes [3]. Nature

722   115, 494–495. https://doi.org/10.1038/115494b0

723   Shichida, Y., Matsuyama, T., 2009. Evolution of opsins and phototransduction. Philos. Trans. R.

724   Soc. B Biol. Sci. 364, 2881–2895. https://doi.org/10.1098/rstb.2009.0051

725   Soni, B.G., Philp, A.R., Foster, R.G., Knox, B.E., 1998. Novel retinal photoreceptors [3]. Nature

726   394, 27–28. https://doi.org/10.1038/27794

727   Stevenson, T.J., Ball, G.F., 2012. Disruption of neuropsin mRNA expression via RNA

728   interference facilitates the photoinduced increase in thyrotropin-stimulating subunit β in

729   birds. Eur. J. Neurosci. 36, 2859–2865. https://doi.org/10.1111/j.1460-9568.2012.08209.x

730   Stevenson, T.J., Bernard, D.J., Ball, G.F., 2009. Photoperiodic condition is associated with

731   region-specific expression of GNRH1 mRNA in the preoptic area of the male starling

732   (Sturnus vulgaris). Biol. Reprod. 81, 674–680.

733   https://doi.org/10.1095/BIOLREPROD.109.076794

734   Stevenson, T.J., Hahn, T.P., Macdougall-Shackleton, S.A., Ball, G.F., 2012. Gonadotropin-

735   releasing hormone plasticity: A comparative perspective. Front. Neuroendocrinol. 33, 287–

736   300. https://doi.org/10.1016/j.yfrne.2012.09.001

737   Stevenson, T.J., Liddle, T.A., Stewart, C., Marshall, C.J., Majumdar, G., 2022. Neural

738   programming of seasonal physiology in birds and mammals: A modular perspective. Horm.

739   Behav. 142. https://doi.org/10.1016/j.yhbeh.2022.105153

740   Wickham, H., Averick, M., Bryan, J., Chang, W., McGowan, L.D., François, R., Grolemund, G.,

741   Hayes, A., Henry, L., Hester, J., 2019. Welcome to the Tidyverse. J. Open Source Softw. 4,

742   1686.

743   Yamamura, T., Hirunagi, K., Ebihara, S., Yoshimura, T., 2004. Seasonal Morphological Changes

744   in the Neuro-Glial Interaction between Gonadotropin-Releasing Hormone Nerve Terminals

745   and Glial Endfeet in Japanese Quail. Endocrinology 145, 4264–4267.

746   https://doi.org/10.1210/en.2004-0366

747

Statements and Declarations

749

Funding

755

Competing Interests

757 The authors have no relevant competing financial or non-financial interests to disclose.

758

Author Contributions

760 TJS, SLM, ICD and RGF conceived of the initial study design. TJS, SLM and ICD secured and
761 provided the grant funding for the experiments described. JHP, TJS, SLM and ICD refined initial
762 experimental design. JHP carried out the experiments with SLM. JHP conducted all
763 morphometric data collection. JHP, ET, VRB, and TJS conducted the molecular lab work. TJS
764 and SNP designed the shRNAi sequences. RGF provided initial antibody stocks. JHP conducted
765 the statistical analysis and drafted the main manuscript. All authors contributed to revision and
766 editing of the draft manuscript prior to final submission

767

Data Availability

769 Data and analytic code (text format) for R analyses are provided in the supplementary files. For
770 the purpose of open access, the author has applied a CC BY public copyright license to any
771 Author Accepted Manuscript version arising from this submission.
772

773 **Ethics Approvals**

774 Animal procedures were approved by the Roslin Institute Animal Ethics and Welfare Review
775 Board at the University of Edinburgh and were performed under Home Office approval (PPL
776 P61FA9171). The experiments were designed in accordance with the Animal Research
777 Reporting of In Vivo Experiments (ARRIVE) guidelines and National Centre for the
778 Replacement, Refinement and Reduction of Animals in Research.
779

780

Figures
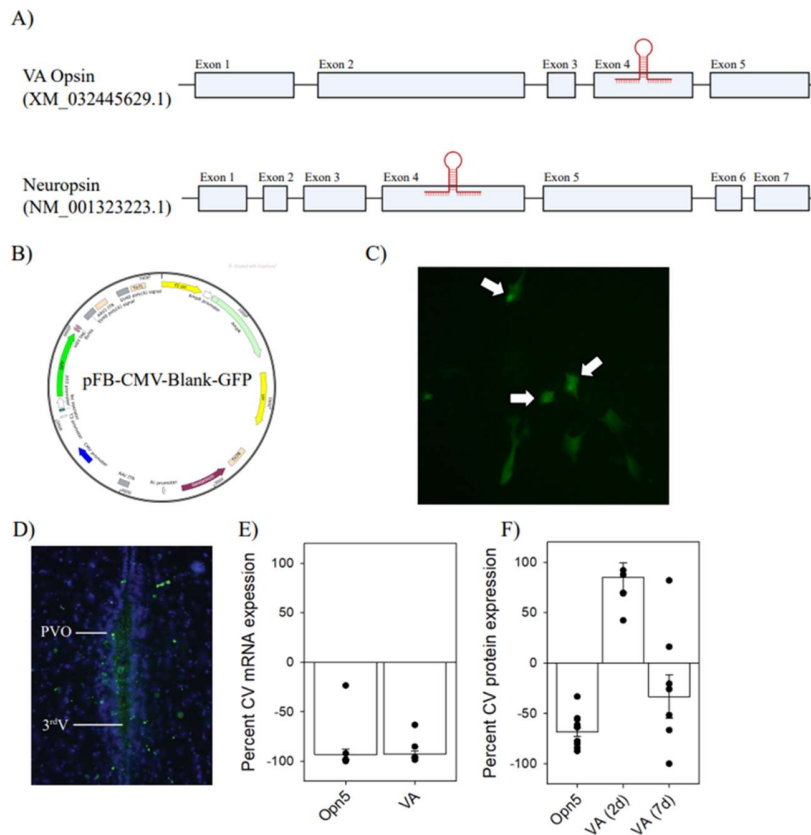
Fig. 1. Specificity and effectiveness of photoreceptor RNA interference

Specificity of RNA interference (RNAi) was achieved by designing probes that target Exon 4 in both VA opsin and Neuropsin (OPN5) sequences (A). Plasmids included a CMV promoter and green fluorescent protein (GFP). shRNAi vectors for VA opsin or OPN5 were inserted upstream to the CMV promoter, blank 'control' plasmid is shown (B). Primary cell culture of embryonic Japanese quail (E10) cells were used to confirm transduction capacity of AAV2 viral serotypes. Cells cultured with 2ul of AAV2 blank constructs showed robust transfection indicated by the white arrows (C). Representative photomicrograph of a coronal section through the mediobasal hypothalamus with the Periventricular organ (PVO) showing strong fluorescence. GFP expression was used to confirm the anatomical localization of intracerebroventricular injection of shRNAi constructs and presence of transfected cells 6-weeks after surgery (D). qPCR and western-blot assays were conducted to establish the effectiveness of shRNAi to reduced mRNA (E) and protein (F) expression for OPN5 and VA opsin. OPN5 mRNA and protein showed highly-effective reduction in photoreceptor expression. shRNAi against VA opsin induced a near 100% reduction in expression. VA opsin protein levels are shown separately for 2 day and 7-day treatment groups to highlight the variation across conditions. Higher VA opsin protein levels observed in 2-day birds likely reflects increased translation of VA opsin mRNA reserves or a transient disruption in the homeostatic balance of photoreceptor levels.
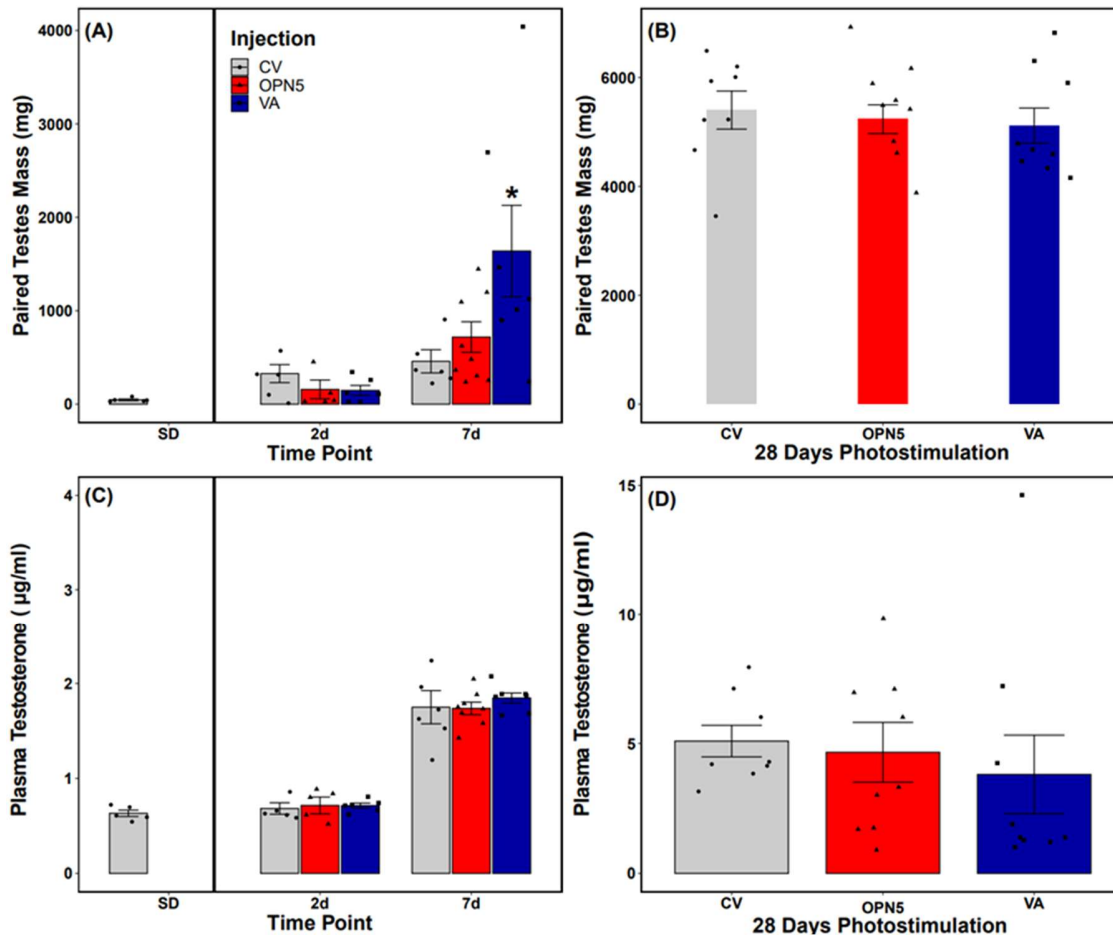
Fig 2. Effects of acute and chronic opsin silencing on opsin expression.

Effects of acute (A) or 28-day chronic (B) shRNAi knockdown of vertebrate ancient opsin (VA) and neuropsin (OPN5) compared to control AAV2 vector cassette (CV) on paired testes mass in Japanese quail reveals VA knockdown leads to accelerated induction of testes growth after 7 days of photostimulation (16L:8D). Plasma testosterone, (µg/ml) measured by ELISA, was unaffected by either acute (C) or 28-day chronic (D) opsin silencing, but increased with duration of photostimulation from acute to chronic. Asterisk (*) indicate $p < 0.05$ significant differences from control birds within the given time point. All values plotted as mean $\pm$ sem.
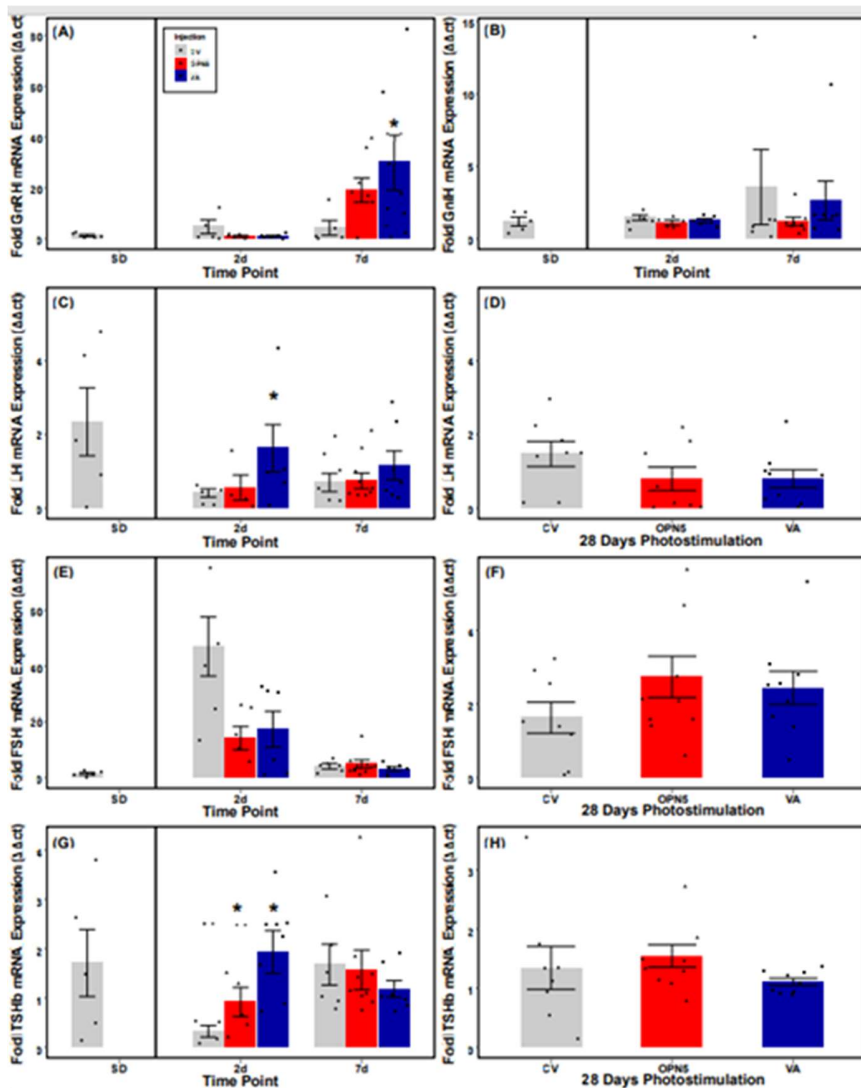
819

820

Fig 3. Photoinduced neuroendocrine gene expression.

Gene expression measured by RT-qPCR in control (CV) and vertebrate ancient opsin (VA) and neuropsin (OPN5) silenced quail for GnRH-I (A), GnIH (B), acute LH (C), 28-day chronic LH (D), acute FSH (E), 28-day chronic (F), acute TSHβ (G) and 28-day chronic TSHβ (H). Knockdown treatment induced increased TSHβ expression during the early photoinducible phase (2D) in both OPN5 and VA silenced animals, but only VA opsin knockdown effected gonadotroph expression with increased LH expression at 2 days and subsequently increased GnRH-I expression at 7 days of photostimulation. Asterisk (*) indicate $p < 0.05$ significant differences from control birds within the given time point. All values plotted as mean $\pm$ sem. Removed outliers are shown as black points, except in panel C where an outlier, value 10.52, in the CV at 2 days was removed.

832

833

834

835
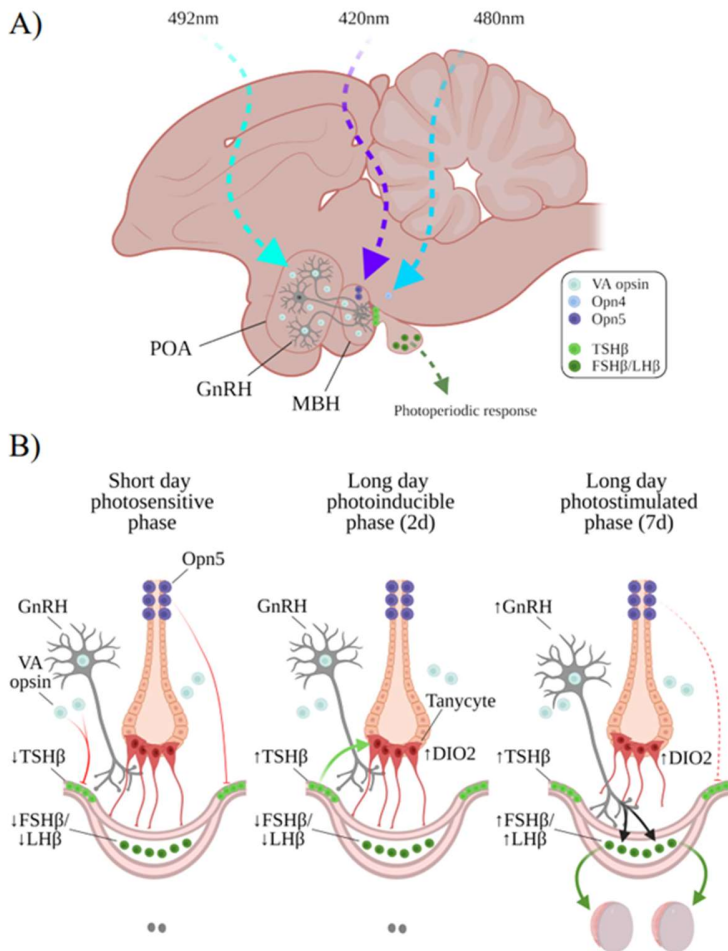
Fig 4. Schematic representation of the photoperiodic control of the neuroendocrine axis in birds. (A) Multiple wavelengths of light penetrate deep into the quail brain and are detected by at least three photoreceptors: vertebrate ancient opsin (VA opsin; λ492), neuropsin (OPN5; λ420) and melanopsin (OPN4; λ480). VA opsin is widely distributed in the preoptic area (POA) and mediobasal hypothalamus (MBH). OPN5 is localized to the PVO in the MBH and OPN4 is sparsely distributed in the MBH. Gonadotropin-releasing hormone (GnRH-I) neurons project from the preoptic area into the MBH to stimulate the release of luteinizing hormone (LH) and follicle-stimulating hormone (FSH). (B) Short day birds maintain regressed gonads due to an inability of GnRH-I neurons to contact the basal lamina membrane that separates the median eminence from the pituitary gland. Photoinduction by long days activates VA opsin and OPN5 cells located in the POA and mediobasal hypothalamus. Two- days light stimulation of VA opsin and OPN5 facilitated *TSHβ* expression. After 7 days of photostimulation of VA opsin either directly co-expressed in GnRH-I neurons or indirectly (via disinhibition from VA neurons) resulted in higher *GnRH* expression. GnRH-I access to the basal lamina permits that ability to stimulate gonadotropin release from the pituitary and trigger gonadal growth.

Supporting information

S1 Figure. 28 LD Testes histology and gene expression measured by qPCR. Gene expression metrics include Androgen Receptor (A), LH Receptor (B), and FSH Receptor (C). All gene expression values presented as fold expression using $\Delta\Delta$CT method as describe in main text with GAPDH and β-Actin reference genes. Testes histology for Sox9 as a Sertoli cell marker (D), total number of tubules (E), and Sox9 positive cell to tubule ratio (F). For each testes marker treatment effect was analyzed by linear model. Line with "*" indicates a significant difference between treatment and control group $p < 0.05$.

S1 Table. AAV2 shRNA sequences used to suppress neuropsin and VA opsin expression

S2 Table. qPCR primers used for Japanese quail hypothalamus and annealing temperatures.

S3 Table. Antibody target and sequence for immunohistochemistry and western blot

S2 File. R analytic code and data file. The R code used for all analyses and figures presented in main and supporting documents as well as raw data file used in the analysis presented in a PDF format.